

Computational Analysis of Knee Joint Stability Following Total Knee Arthroplasty Using Bode Margins

Marzieh M Ardestani¹, ZhenXian Chen², Hessam Noori³, Mehran Moazen⁴, Zhongmin

Jin^{2,5,6}

¹Department of Physical Medicine and Rehabilitation, School of Medicine,
Indiana University, IN, USA

² School of Mechanical Engineering, Southwest Jiaotong University, Chengdu, China

³ School of Mechanical and Energy Engineering, Purdue University, Purdue, IN

⁴Department of Mechanical Engineering, University College London, Torrington Place,
London WC1E 7JE, UK

⁵ School of Mechanical Engineering, Xian Jiaotong University, Xian, China

⁶School of Mechanical Engineering, University of Leeds, Leeds, LS2 9JT, UK

*Address for corresponding author:

Marzieh M. Ardestani

Assistant Research Professor

Department of Physical medicine and Rehabilitation

School of Medicine

Indiana University-Purdue University

4141 Shore Dr

Indianapolis, IN, 46254

Email: mamost@iu.edu

1 **Abstract**

2 The overall objective of this study was to introduce knee joint power as a potential measure to
3 investigate knee joint stability following total knee arthroplasty (TKA). Specific aims were to investigate
4 whether weakened knee joint stabilizers cause abnormal kinematics and how it influences the knee joint
5 kinetic (i.e., power) in response to perturbation.

6 Patient-specific musculoskeletal models were simulated with experimental gait data from six TKA
7 patients (baseline models). Muscle strength and ligament force parameter were reduced by up to 30% to
8 simulate weak knee joint stabilizers (weak models). Two different muscle recruitment criteria were tested
9 to examine whether altered muscle recruitment pattern can mask the influence of weakened stabilizers on
10 the knee joint kinematics and kinetics. Level-walking knee joint kinematics and kinetics were calculated
11 through force-dependent kinematic and inverse dynamic analyses. Bode analysis was then recruited to
12 estimate the knee joint power in response to a simulated perturbation.

13 Weak models resulted in larger anterior-posterior (A-P) displacement and internal-external (I-E)
14 rotation compared to baseline (I-E: 18.4 ± 8.5 vs. 11.6 ± 5.7 (deg), A-P: 9.7 ± 5.6 vs. 5.5 ± 4.1 (mm)). Changes
15 in muscle recruitment criterion however altered the results such that A-P and I-E were not notably different
16 from baseline models. In response to the simulated perturbation, weak models versus baseline models
17 generated a delayed power response with unbounded magnitudes. Perturbed power behavior of the knee
18 remained unaltered regardless of the muscle recruitment criteria.

19 In conclusion, impairment at the knee joint stabilizers may or may not lead to excessive joint
20 motions but it notably affects the knee joint power in response to a perturbation. Whether perturbed knee
21 joint power is associated with the patient-reported outcome requires further investigation.

22
23

24 **Keywords:** Total knee arthroplasty, instability, knee kinematics, gait, Bode analysis

25 **1. Introduction**

26 Instability of total knee arthroplasty (TKA) causes 20-30% of the implanted knees to be revised
27 annually (Parratte and Pagnano, 2008; Rodriguez-Merchan, 2011). Accurate diagnosis is therefore
28 crucial to plan the revision surgery (Kanamiya et al., 2002; Matsuda and Ito, 2015). However, the
29 diagnosis can be challenging; e.g., 8-20% of TKA patients complain about persistent instability in
30 the absence of any immediate symptoms (Azzam et al., 2011; Sharkey et al., 2014; Song et al.,
31 2014). Persistent, yet asymptomatic, knee instability is often attributed to insufficiency of the knee
32 joint stabilizers; i.e., lax ligaments and/or weak muscles. Impaired knee joint stabilizers can cause
33 abnormal, often unbounded kinematics and/or kinetics in response to a bounded perturbation
34 (Bergmark, 1989).

35 Hypermobility, i.e., excessive anterior-posterior (A-P) displacement (Fantozzi et al., 2006;
36 Stoddard et al., 2013) and/or internal-external (I-E) rotation (Wautier and Thienpont, 2017;
37 Zaffagnini et al., 2014) is a familiar manifest of the unbounded kinematic response of an unstable
38 knee. Yet, whether the diagnosis of instability should be excluded when hypermobility is not
39 observed during clinical assessments is a matter of debate (Martín-Hernández et al., 2014;
40 Nakahara et al., 2015).

41 Classic clinical assessments of hypermobility such as anterior drawer test, Lachman evaluation
42 and pivot shift test apply subjective perturbations (Athwal et al., 2014). Recent studies
43 recommended alternative evaluations of the knee joint kinematics under a more dynamic condition
44 such as level walking or stair navigation to evoke hypermobility (Denney et al., 2014; Joglekar et
45 al., 2012; Soeno et al., 2018). Nonetheless, human neuro-musculoskeletal system is capable of
46 adopting a compensatory muscle recruitment strategy (i.e., redundancy) such that kinematic and
47 kinetic behavior, especially in a low-demanding task such as level-walking, remains unaltered

48 (Bonnefoy-Mazure et al., 2017; Liebensteiner et al., 2008; Soeno et al., 2018). Our recent study
49 showed that TKA patients with sub-optimal knee function may still demonstrate asymptomatic
50 knee kinematics, owing to compensatory muscle recruitment patterns (Ardestani et al., 2017).

51 Abnormal kinetic behavior in response to perturbation, e.g., unbounded joint power can be
52 another manifest of instability (Levin et al., 2015; Vera-Garcia et al., 2007). This concept however
53 is overlooked in TKA studies. One explanation can be that any perturbation may damage the
54 prosthetic knee and thus may not be applied due to ethical considerations. Besides, the
55 perturbation, required to evoke the unbounded behavior, might be patient-specific. Bode analysis
56 is a well-documented technique in control engineering (Ogata and Yang, 2002) capable of
57 simulating a perturbation and then qualitatively estimating the perturbed behavior of a system to
58 determine its stability margins, often referred as “Bode margins” . Bode analysis estimates the
59 perturbed behavior of a system based on its unperturbed dynamic(Dorf and Bishop, 2011), and
60 thus relaxes the necessity of applying an actual perturbation to the system (i.e., the knee joint).
61 Additionally, Bode analysis often simplifies a complex system to a linear function with few inputs
62 and outputs. For instance, the knee joint can be modeled as a linear function with the knee joint
63 kinematics and kinetics as inputs and the knee joint power as output facilitating the estimation of
64 the perturbed knee joint power. Bode analysis was recently used to estimate the perturbed
65 kinematic behavior of unstable knees following anterior-cruciate ligament injury (Morgan et al.,
66 2016).

67 The overall objective of this study was to investigate the applicability of Bode analysis to
68 estimate the perturbed knee joint power in TKA patients. We aimed to investigate whether
69 weakened knee joint stabilizers cause abnormal kinematics during walking (hypermobility) and

70 how it can influence the knee joint kinetics (power) in response to larger perturbations beyond
71 level-walking.

72 **2. Materials and Methods**

73 Six TKA patients were obtained from a published repository (Section 2.1). Our previously
74 published musculoskeletal (MSK) model of a typical TKA patient was scaled to each patient
75 (Section 2.2). Two separate versions of MSK models were developed: (i) baseline (BSL) models
76 with intact joint stabilizers (muscles and ligaments) and (ii) weakened (WEAK) models for which
77 the knee muscle strength and ligament force parameter were reduced. For each patient, BSL and
78 WEAK models were simulated with the averaged level-walking gait profile (ground reaction force
79 and marker trajectories) of that patient. Inverse dynamic and Force-dependent kinematic (FDK)
80 analyses were conducted to calculate knee joint kinetics and the secondary knee joint kinematics
81 (A-P displacement and I-E rotation) respectively. This was performed to investigate whether
82 weakened knee joint stabilizers immediately lead to abnormal pattern in the secondary knee joint
83 kinematics (hypermobility). The knee joint kinematics and kinetics from BSL and WEAK models
84 were then imported to Bode analysis to estimate the knee joint power in response to the simulated
85 perturbation (Section 2.3). This was performed to investigate whether weakened joint stabilizers
86 can impact stability margins of the knee joint in response to the perturbation. Figure 1 demonstrates
87 the workflow of the present study.

88 **2.1. Experimental Gait Data**

89 Gait data including ground reaction forces (GRF) and marker trajectories from six TKA
90 patients (5 M/ 1F, Height: 170.8 ± 5.2 cm; Weight: 69.7 ± 4.4 kg) were obtained from a published
91 repository (<https://simtk.org/home/kneeloads>, accessed Sept 2015). TKA patients were implanted
92 with cruciate-retaining sensor-based knee prostheses which measures *in vivo* knee forces. GRFs
93 were recorded at a frequency of 1000 Hz (Force plate, AMTI Corp., Watertown, MA, USA) and
94 marker trajectory data were recorded at a frequency of 200 Hz (10-camera motion capture system,
95 Motion Analysis Corp., Santa Rosa, CA, USA) using a modified Cleveland Clinic marker set with
96 extra markers on the feet and trunk. For a complete description of this database see (Fregly et al.,
97 2012; Kinney et al., 2013).

98 **2.2. Musculoskeletal Model**

99 We previously modified a 3D musculoskeletal model, i.e., Twente Lower Extremity Model
100 (TLEM) model (Horsman, 2007), from AnyBody software repository (version 6.0; AnyBody
101 Technology, Aalborg, Denmark) to represent a TKA patient(Chen et al., 2016a; Chen et al., 2015;
102 Chen et al., 2014; Chen et al., 2016b). TLEM, with 160 muscle-tendon actuators, spherical hip
103 and revolute knee and ankle joints were modified as follows: The generic geometry of the knee
104 (femoral and tibial components) was replaced with the geometry of the knee implant (Figure 2).
105 Two deformable contact models were defined between the tibial insert and femoral component
106 bearing surfaces and between the patellar button and the femoral component. A friction coefficient
107 of 0.04 was considered between the two components (Hashemi et al., 2000). Details of these
108 contact models are discussed in the Appendix. This model solves the equilibrium equations in
109 three dimensions(Damsgaard et al., 2006). The model showed acceptable accuracy in predicting
110 muscle activations and the knee joint contact forces when compared versus in-vivo measurements

111 (Chen et al., 2014; Peng et al., 2018). This model was also used for a series of parametric and
 112 probabilistic studies (Ardestani and Moazen, 2016; Chen et al., 2015). Here, this model was used
 113 to simulate muscle weakness (strength decline) and ligament laxity (decline in ligament force
 114 parameter) and calculate the resultant knee joint kinematics and kinetics.

115 The MSK model was scaled to each patient as follows: model was scaled to each patient's
 116 weight and height using Length–Mass–Fat scaling law(Lund et al., 2015). Body segment lengths
 117 and the relative positions of joints were determined such that the model's markers closely tracked
 118 the experimental marker trajectories. Maximum isometric voluntary contractions of muscles (F_0)
 119 were also scaled using Height-Squared law(Rasmussen et al., 2005). Muscle attachment and
 120 geometries were scaled based on linear geometry scaling law (Worsley et al., 2011). Muscle
 121 strength was represented using a bilinear model (Lloyd and Besier, 2003):

$$122 \quad Strength = F_0 \left(2 \frac{L_m}{L_f} - 1 \right) \left(1 - \frac{L'_m}{V_0} \right) \quad (1)$$

123 Where F_0 is the strength of the muscle at neutral fiber length (L_f) and contraction velocity (L'_m)
 124 equals to zero. L_m is the current length of the contractile element and V_0 is the contraction velocity
 125 at maximum voluntary contraction. F_0 is related to muscle isometric strength and has been
 126 estimated from cadaveric studies (Horsman, 2007) Muscle weakness was simulated by reducing
 127 the strength parameter, F_0 for the following muscles : semimembranosus, semitendinosus, biceps
 128 femoris, rectus femoris, vastus, tibialis anterior , medial gastrocnemius and soleus.

129 Ligaments, including posterior cruciate ligament (PCL), medial collateral ligament (MCL), lateral
 130 collateral ligament (LCL), posteromedial capsule (PMC), medial PF ligament (MPFL), and lateral
 131 PF ligament (LPFL), were modeled as non-linear spring elements with the piecewise force–

132 displacement relationship (Blankevoort, 2001) (Note: anterior cruciate ligament (ACL) was not
 133 modeled considering the surgical removal of this ligament):

$$134 \quad f = \begin{cases} S_0 \times \left(\frac{\varepsilon^2}{4\varepsilon_l}\right) & 0 < \varepsilon < 2\varepsilon_l \\ S_0 \times (\varepsilon - \varepsilon_l) & \varepsilon > 2\varepsilon_l \\ 0 & \varepsilon < 0 \end{cases} \quad (2)$$

$$135 \quad \varepsilon = \frac{L-L_0}{L_0} \quad , \quad L_0 = \frac{L_r}{\varepsilon_r+1} \quad (3)$$

136 where f is the ligament force and S_0 is the ligament force parameter, expressed in newton, ε_l is a
 137 constant non-linear strain parameter of 0.03, ε is the strain in the ligaments, L is the ligament
 138 length, and L_0 is the zero-load length of the ligament (determined from the ligament's initial length
 139 L_r and the reference strain ε_r). Ligament laxity was simulated by reducing ligament force
 140 parameter, S_0 , in equation (2).

141 From each patient-specific model, 400 versions were generated including (i) 100 BSL
 142 models, for which muscle strength and ligament force parameter were chosen from a normal
 143 distribution of the nominal values for that subject $\pm 5\%$ (Amiri and Wilson, 2012), (ii) 100 WEAK
 144 models where F_0 was chosen from a normal distribution of nominal strength reduced by 30% (Silva
 145 et al., 2003). Note our previous study showed reduction beyond 40% can alter the normal gait
 146 pattern (Ardestani and Moazen, 2016); (iii) 100 WEAK models with lax ligaments where S_0 was
 147 chosen from normal distribution of nominal values reduced by 30%. This is consistent with
 148 previous literature reporting up to 30% of variation in ligament stiffness amongst TKA subjects
 149 with unstable knees (Reinders et al., 2014) which may in turn lead to 2 standard deviation in
 150 secondary knee joint kinematics from the average (Kang et al., 2017). Note previous studies
 151 showed that reduction beyond 50% can alter the joint load (Li et al., 2002; Orozco et al., 2018),

152 (vi) 100 WEAK models with both weak muscles and lax ligaments. For BSL models, F_0 and S_0
153 values were consistent with reported values for stable knees (Anderson and Pandy, 1999; Lin et
154 al., 2010) - Table 1). For each patient, both BSL and WEAK models were simulated with the
155 average marker trajectory and GRF profile of the same patient. Inverse dynamic analysis was
156 conducted to calculate the joint moments and muscle forces from GRF and primary joint
157 kinematics. Furthermore, force-dependent kinematic (FDK) analysis was conducted to calculate
158 the secondary knee joint kinematics and internal joint contact forces. For FDK analysis, please see
159 (Andersen et al., 2011). In brief, FDK analysis was conducted by introducing an additional
160 kinematic driver to a standard inverse dynamic analysis. The kinematic driver was the function of
161 joint coordination and time. This was added to represent the fact that in a nonconforming joint
162 such as knee, internal forces influence joint secondary kinematics. The time-derivate of this
163 kinematic drive was assumed to be zero so that the equilibrium equations become quasi-static. The
164 underlying assumption of FDK analysis was that the secondary knee motions were not influenced
165 by the global model dynamics and therefore, can be solved assuming quasi-static equilibrium
166 between ligament, muscle, contact forces, and external loads.

167 Two different muscle recruitment criteria were implemented: (1) the conventional Min-Max
168 optimization which activates the muscles such that minimizes the maximum muscle
169 activation(Marra et al., 2015); (2) a recently proposed synergy optimization which activates
170 muscles to minimize synergy activations (instead of muscle activation) where synergy is defined
171 as phase-specific groups of agonist muscles (Aoi and Funato, 2016; Sartori et al., 2013). Presented
172 by new evidence and confirmed by our recent study (Ardestani et al., 2017), synergistic
173 recruitment of muscles enables the MSK system to accommodate certain levels of muscle
174 weakness and maintain asymptomatic joint kinematics. Therefore, the latter optimization was

175 implemented to investigate whether changes in muscle recruitment pattern can mask muscle
176 weakness and prevent the manifest of abnormal knee kinematics during level-walking.

177 **2.3. Bode Analysis**

178 For the purpose of Bode analysis, knee joint was represented as a linear model with sagittal
179 knee angular velocity and sagittal knee joint moment as inputs and knee joint power as output.
180 Two-thirds of the BSL simulations were used to construct this model and the remaining one-third
181 of BSL simulations were used to validate it. At least 85% accuracy ($R^2 \geq 0.85$) between the knee
182 joint power (output) calculated from the linear model and MSK model was required to deem the
183 linear model of knee as acceptable. This process was conducted using System Identification
184 Toolbox (MATLAB software. 2014b, Chicago, USA).

185 Once the knee joint was formulated, the inputs (motion and moment) were perturbed and the
186 model was recruited to predict the knee joint power (output) in response to the perturbed inputs.
187 Perturbation was modeled as a sudden change in the knee joint motion and/or moment. The ratio
188 of the resultant knee joint power in response to the perturbed knee flexion angle and/or moment
189 was calculated and referred as “*amplitude response*”. The temporal delay between when the
190 perturbation occurred in the input and when the knee joint responded, was also calculated and
191 referred as “*phase response*”.

192 Amplitude and phase responses of the knee joint was calculated across a range of different
193 perturbations (frequencies) and was considered as “frequency response” of the knee joint. Bode
194 plot displays the amplitude response vs. frequency and the phase response vs. frequency of the
195 knee joint (Figure 3). Stability margins were obtained from the Bode plot, namely (1) gain margin
196 and (2) phase margin (Figure 3):

197 $\text{Gain Margin} = 0 - G$ (4)

198 where G is the amplitude response of the knee joint in decibel (dB) at a perturbation for which
199 the phase response of knee joint equals to -180 deg indicating that knee generated the power with
200 half a cycle delay in response to perturbation.

201 $\text{Phase Margin} = +P + 180$ degrees (5)

202 where P is the phase response of the knee joint (in degrees) at a perturbation for which its amplitude
203 response equals to 0 dB indicating that the output and input amplitudes of the knee joint are equal.
204 As suggested in control engineering, negative amplitude margin and/or negative phase margin
205 indicate an unstable system (Dorf and Bishop, 2011; Ogata and Yang, 2002).

206 **3. Results**

207 **3.1.Secondary Knee Joint Motions in BSL vs. WEAK models**

208 FDK analyses of BSL models, with nominal muscle strength and ligament force parameter,
209 led to an average I-E rotation of 11.6 ± 5.7 (deg) and A-P displacement of 5.5 ± 4.1 (mm). FDK
210 analyses of models with weak muscles (Figure 4) led to slightly higher I-E rotation (15.7 ± 8.4
211 (deg)) and A-P displacement (8.3 ± 5.8 (mm)). Models with lax ligaments also led to larger knee
212 joint motions (I-E: 15.3 ± 5.4 (deg), A-P: 6.7 ± 5.7 (mm)). Models with simultaneous muscle
213 weakness and ligament laxity resulted in even larger ranges of knee motions (I-E: 18.4 ± 8.5 (deg),
214 A-P: 9.7 ± 5.6 (mm)). Switching the cost function from Min-Max to synergy optimization changed
215 the muscle recruitment patterns and thus the secondary motions of the knee joint such that results
216 were not notably different from BSL MSK models (Figure 4 and Table 2).

217 Note, WEAK models compared to BSL models led to large standard deviations in the knee
218 joint motion. Subset analyses of models showed that only models with the reduction in muscle

219 strength by 30%, or reduction in ligament force parameter by 18% caused recognizable deviation
220 (i.e., more than one std) from BSL models. WEAK models with simultaneous reduction in muscle
221 strength (>24%) and in ligaments force parameter (>15%) led to even larger kinematic deviation
222 from BSL models. In this subset of MSK models, switching the cost function from Min-Max to
223 synergy optimization decreased the kinematic deviations but the kinematics remained marginally
224 significant from BSL models (Table 2).

225 **3.2.Bode Margins in BSL vs. WEAK Models**

226 Bode analysis of all BSL models led to positive stability margins (i.e., positive amplitude
227 margin and positive phase margin) with amplitude margins (G) ranging from 5.8(dB) to 22.5(dB)
228 and phase margins (P) ranging from 35.7 (deg) to 136.8(deg) indicating a promptly-generated
229 power with bounded amplitude in response to perturbation (Figure 5a). In contrast, 85% of WEAK
230 models with reduced muscle strength, ligament force parameter or both led to negative stability
231 margins in Bode analysis. More directly, 88% of WEAK models with reduced muscle strength
232 led to negative amplitude margins ($G = -15.8 \pm 13.5$ (dB)) indicating an unbounded power response
233 to perturbation (Figure 5b). On the other hand, 82% of WEAK models with reduced ligament force
234 parameter led to negative phase margins ($P = -65.3 \pm 23.7$ (deg)) indicating a delayed power
235 behavior in response to perturbation (Figure 5c). Note 12% of models with reduced muscle
236 strength and 18% of those with reduced ligament force parameter still led to positive, albeit small,
237 stability margins ($G = 2.3 \pm 2.7$ (dB), $P = 11.4 \pm 6.9$ (deg)). A closer investigating of these models
238 revealed that manipulated parameters were close to nominal thresholds (strength reduction less
239 than 10% and ligament force parameter reduction less than 8%). Switching the cost function from
240 Min-Max to synergy optimization decreased the prevalence of negative stability margins from
241 88% to 72% (and from 82% to 78%) in models with reduced strength (and models with reduced

242 ligament force parameter). Yet, the prevalence of negative Bode margins in WEAK models
243 remained notable.

244 Bode analyses of WEAK models with simultaneous reductions of muscle strength and
245 ligament force parameter led to negative stability margins indicating a delayed ($P=-97.8\pm 32$ (deg))
246 and unbounded ($G=-23.8\pm 14.6$ (dB)) power response to perturbation (Figure 5d). In these models,
247 Bode estimations of the knee power were consistent regardless of the muscle recruitment function;
248 i.e., changing the muscle recruitment function from the Min-Max optimization to the synergy
249 optimization slightly changed the magnitude and the delay in joint power, but WEAK models still
250 showed a delayed power behavior with unbounded magnitude in response to perturbation (see
251 Figure 5). Samples of Bode plots are presented in the Appendix.

252 **4. Discussion**

253 This study recruited Bode analysis to qualitatively estimate the knee joint power in response
254 to a simulated perturbation. We aimed to investigate whether weakness (up to 30%) in the ligament
255 and muscles immediately cause abnormal knee kinematics during level walking (hypermobility)
256 and whether impair the kinetic behavior (power) in response to the larger perturbations. Two
257 different muscle recruitment criteria were also tested to examine whether altered muscle
258 recruitment pattern can mask the influence of weak stabilizers on the knee joint kinematics and
259 kinetics. Results showed that depending on the muscle recruitment pattern, weak knee joint
260 stabilizers may or may not cause excessive joint motions, but it notably affects the knee joint power
261 in response to the perturbation.

262 Computational analyses of the knee joint stability advance our understanding of the
263 isolated and combined roles of knee joint kinematics and kinetics, muscle co-activation or

264 anatomical variables on the knee joint stability (Sharifi et al., 2018). Significant reduction in
265 ligament stiffness and/or muscle activation has been shown to change the knee joint kinematics
266 and causes hypermobility (Sharifi et al., 2017). Some patients however may demonstrate
267 asymptomatic knee kinematics during walking while presenting with persistent complaints of knee
268 instability and dysfunction (Ardestani et al., 2017). The present study therefore focused on only
269 small levels of muscle weakness and ligament laxity. Considering the redundancy of human MSK
270 system, we aimed to demonstrate that impairment at the knee stabilizers may be compensated
271 through altered muscle recruitment such that it may not immediately translate into abnormal
272 kinematics. Yet, it may impair the ability of the knee joint to respond to a perturbation beyond
273 level walking. Morgan et al used Bode analysis to discuss the abnormal knee kinematic in response
274 to perturbation and the present study focused on perturbed kinetic behavior.

275 The knee joint power was studied as the kinetic behavior of interest. The knee joint power
276 integrates the role of both kinematics (dictated by passive constraints such as ligaments) and
277 kinetics (dictated by active constraints i.e., muscles) and hence is expected to be more informative
278 to manifest knee joint complications. Besides, the knee joint power is calculated as the dot product
279 of the joint moment and the angular velocity (the derivation of sagittal knee motion). Sagittal knee
280 joint motion is the dominant movement of the knee joint and mid-flexion instability is the most
281 popular type of instability. Moreover, daily-life activities often induce perturbation which can be
282 modeled as sudden changes in the movement (e.g., rapid turn) and/or sudden changes in the ground
283 reaction forces (e.g., uneven ground, slippery surfaces) influencing the knee joint moment.

284 This study has several limitations. First the computational approach was based on a small
285 patient population. Nonetheless, random selection of the key variables including muscle strength
286 and ligament force parameter created a large probabilistic data base (400 simulations per each

287 subject). Future experimental investigations with a larger TKA population is required to confirm
288 present findings.

289 Second, computational modeling including MSK modeling and Bode analysis bring their
290 inherent limitations. The origin and insertion sites of the muscles and the ligaments were based on
291 TLEM model and may not exactly represent individual patients. Although MSK models were
292 scaled to each patient, other properties such as muscle activation, muscle cross-sectional area and
293 ligament geometries were not adjusted to individual age and their unique anatomy. Moreover,
294 muscle weakness was solely simulated by decreasing the strength. Reduction in muscle cross-
295 sectional area and muscle fiber excitability are other etiologies that may also lead to muscle
296 weakness. Also, muscle weakness was only simulated in eight muscles. It should be noted that
297 other muscles, even those that are not directly connected to the knee, may also influence the knee
298 joint loads and its motions. Muscle-tendon units were simplified using a bilinear model (equation
299 1). This model consists of a contractile element and a serial-elastic element. Unlike a hill-type
300 model, the bilinear model does not have a parallel elasticity element to account for passive muscle
301 force. Instead, this model uses larger isometric force parameters compared to hill-type model To
302 account for passive muscle force. This built-in passive force however cannot be switch off and
303 may leads to over-estimated muscle strength and thus muscle forces. This model was chosen as it
304 is computationally efficient for probabilistic studies.

305 Furthermore, the knee joint stabilizers (ligaments and muscles) were weakened according to
306 pre-determined thresholds and from a normal probability distribution. These assumptions may not
307 necessarily represent an “unstable knee” but rather an increased likelihood of instability. Note,
308 both BSL and WEAK models were simulated using the same marker trajectory data. Therefore
309 knee F-E rotation and the overall kinematic pattern of walking calculated based on marker

310 trajectories were assumed to be the same for both models (Thompson et al., 2013; van der Krogt
311 et al., 2012). In real world however, changes in the joint internal structure can influence all joint
312 kinematics in all planes. Furthermore, Bode analysis simplifies the knee by a linear approximation
313 to computationally simulate perturbation and to qualitatively estimate system's behavior in
314 frequency domain. Bode analysis is not a quantitative approach and interpretation of its result in
315 time domain should be conducted with caution.

316 Finally, further investigations are required to provide a one-by-one comparison between the
317 knee joint power, knee joint kinematic and Bode margins in presence of a real perturbation.
318 Questions such as whether Bode margins are negative (or respectively positive) for patients with
319 confirmed knee instability (or for uninjured knee joints) remains unanswered.

320 In summary this study explored the application of Bode analysis to estimate the knee joint
321 power in response to a simulated perturbation. Impairment at the knee joint stabilizers can
322 potentially impair the knee joint power in response to the perturbation regardless of the muscle
323 recruitment pattern.

324

325 **Conflict of interest**

326 The authors have no financial or non-financial competing interests relevant to this manuscript.

327 **Acknowledgements**

328 Authors would like to include a special note of thanks for Dr Aaron G. Rosenberg and Dr Markus
329 A. Wimmer for contributing their valuable time and thoughts to discuss this topic.

330

331 **References**

- 332 Amiri, S., Wilson, D.R., 2012. A computational modeling approach for investigating soft tissue balancing in
333 bicruciate retaining knee arthroplasty. *Computational and mathematical methods in medicine* 2012.
- 334 Andersen, M.S., Damsgaard, M., Rasmussen, J., Year Force-dependent kinematics: a new analysis method
335 for non-conforming joints. In *XIII International Symposium on Computer Simulation in Biomechanics*,
336 Leuven, Belgium.
- 337 Anderson, F.C., Pandy, M.G., 1999. A dynamic optimization solution for vertical jumping in three
338 dimensions. *Computer methods in biomechanics and biomedical engineering* 2, 201-231.
- 339 Aoi, S., Funato, T.J.N.r., 2016. Neuromusculoskeletal models based on the muscle synergy hypothesis for
340 the investigation of adaptive motor control in locomotion via sensory-motor coordination. 104, 88-95.
- 341 Ardestani, M.M., Malloy, P., Nam, D., Rosenberg, A.G., Wimmer, M.A., 2017. TKA patients with
342 unsatisfying knee function show changes in neuromotor synergy pattern but not joint biomechanics.
343 *Journal of Electromyography and Kinesiology* 37, 90-100.
- 344 Ardestani, M.M., Moazen, M.J.J.o.b., 2016. How human gait responds to muscle impairment in total knee
345 arthroplasty patients: muscular compensations and articular perturbations. 49, 1620-1633.
- 346 Athwal, K.K., Hunt, N.C., Davies, A.J., Deehan, D.J., Amis, A.A., 2014. Clinical biomechanics of instability
347 related to total knee arthroplasty. *Clinical Biomechanics* 29, 119-128.
- 348 Azzam, K., Parvizi, J., Kaufman, D., Purtill, J.J., Sharkey, P.F., Austin, M.S., 2011. Revision of the unstable
349 total knee arthroplasty: outcome predictors. *The Journal of arthroplasty* 26, 1139-1144.
- 350 Bergmark, A., 1989. Stability of the lumbar spine: a study in mechanical engineering. *Acta Orthopaedica*
351 *Scandinavica* 60, 1-54.
- 352 Blankevoort, L.J.J.o.B., 2001. Articular contact in a three dimensional model of the knee. 34, 859-871.
- 353 Bonnefoy-Mazure, A., Armand, S., Sagawa, Y., Suvà, D., Miozzari, H., Turcot, K., 2017. Knee kinematic and
354 clinical outcomes evolution before, 3 months, and 1 year after total knee arthroplasty. *The Journal of*
355 *arthroplasty* 32, 793-800.
- 356 Chen, Z., Jin, Z.J.B., *Biotribology*, 2016a. Prediction of in-vivo kinematics and contact track of total knee
357 arthroplasty during walking. 2, 86-94.
- 358 Chen, Z., Wang, L., Liu, Y., He, J., Lian, Q., Li, D., Jin, Z., 2015. Effect of component mal - rotation on knee
359 loading in total knee arthroplasty using multi - body dynamics modeling under a simulated walking gait.
360 *Journal of Orthopaedic Research* 33, 1287-1296.
- 361 Chen, Z., Zhang, X., Ardestani, M.M., Wang, L., Liu, Y., Lian, Q., He, J., Li, D., Jin, Z., 2014. Prediction of in
362 vivo joint mechanics of an artificial knee implant using rigid multi-body dynamics with elastic contacts.
363 *Proceedings of the Institution of Mechanical Engineers, Part H: Journal of Engineering in Medicine* 228,
364 564-575.
- 365 Chen, Z., Zhang, Z., Wang, L., Li, D., Zhang, Y., Jin, Z.J.M.e., physics, 2016b. Evaluation of a subject-specific
366 musculoskeletal modelling framework for load prediction in total knee arthroplasty. 38, 708-716.
- 367 Damsgaard, M., Rasmussen, J., Christensen, S.T., Surma, E., De Zee, M.J.S.M.P., *Theory*, 2006. Analysis of
368 musculoskeletal systems in the AnyBody Modeling System. 14, 1100-1111.
- 369 Denney, L.M., Ferris, L.A., Dai, H., Maletsky, L.P., 2014. Analysis of a rotary task following total knee
370 arthroplasty: Stair descent with a cross-over turn. *Proceedings of the Institution of Mechanical Engineers*,
371 *Part H: Journal of Engineering in Medicine* 228, 429-438.
- 372 Dorf, R.C., Bishop, R.H., 2011. *Modern control systems*. Pearson.
- 373 Fantozzi, S., Catani, F., Ensini, A., Leardini, A., Giannini, S., 2006. Femoral rollback of cruciate - retaining
374 and posterior - stabilized total knee replacements: in vivo fluoroscopic analysis during activities of daily
375 living. *Journal of orthopaedic research* 24, 2222-2229.

376 Fregly, B.J., Besier, T.F., Lloyd, D.G., Delp, S.L., Banks, S.A., Pandy, M.G., D'Lima, D.D., 2012. Grand
377 challenge competition to predict in vivo knee loads. *Journal of Orthopaedic Research* 30, 503-513.

378 Hashemi, A., Shirazi-Adl, A.J.C.m.i.b., engineering, b., 2000. Finite element analysis of tibial implants—
379 effect of fixation design and friction model. 3, 183-201.

380 Horsman, K., 2007. The Twente lower extremity model. Consistent dynamic simulation of the human
381 locomotor apparatus.

382 Joglekar, S., Gioe, T.J., Yoon, P., Schwartz, M.H., 2012. Gait analysis comparison of cruciate retaining and
383 substituting TKA following PCL sacrifice. *The Knee* 19, 279-285.

384 Kanamiya, T., Whiteside, L.A., Nakamura, T., Mihalko, W.M., Steiger, J., Naito, M., 2002. Effect of Selective
385 Lateral Ligament Release on Stability in Knee Arthroplasty. *Clinical orthopaedics and related research* 404,
386 24-31.

387 Kang, K., Koh, Y., Jung, M., Nam, J., Son, J., Lee, Y., Kim, S., Kim, S.J.B., research, j., 2017. The effects of
388 posterior cruciate ligament deficiency on posterolateral corner structures under gait-and squat-loading
389 conditions: A computational knee model. 6, 31-42.

390 Kinney, A.L., Besier, T.F., D'Lima, D.D., Fregly, B.J., 2013. Update on grand challenge competition to predict
391 in vivo knee loads. *Journal of biomechanical engineering* 135, 021012.

392 Levin, O., Vanwanseele, B., Thijsen, J.R., Helsen, W.F., Staes, F.F., Duysens, J., 2015. Proactive and reactive
393 neuromuscular control in subjects with chronic ankle instability: evidence from a pilot study on landing.
394 *Gait & posture* 41, 106-111.

395 Li, G., Suggs, J., Gill, T.J.A.o.b.e., 2002. The effect of anterior cruciate ligament injury on knee joint function
396 under a simulated muscle load: a three-dimensional computational simulation. 30, 713-720.

397 Liebensteiner, M., Herten, A., Gstoettner, M., Thaler, M., Krismer, M., Bach, C., 2008. Correlation between
398 objective gait parameters and subjective score measurements before and after total knee arthroplasty.
399 *The Knee* 15, 461-466.

400 Lin, Y.-C., Walter, J.P., Banks, S.A., Pandy, M.G., Fregly, B.J., 2010. Simultaneous prediction of muscle and
401 contact forces in the knee during gait. *Journal of biomechanics* 43, 945-952.

402 Lloyd, D.G., Besier, T.F.J.J.o.b., 2003. An EMG-driven musculoskeletal model to estimate muscle forces
403 and knee joint moments in vivo. 36, 765-776.

404 Lund, M.E., Andersen, M.S., de Zee, M., Rasmussen, J.J.I.B., 2015. Scaling of musculoskeletal models from
405 static and dynamic trials. 2, 1-11.

406 Marra, M.A., Vanheule, V., Fluit, R., Koopman, B.H., Rasmussen, J., Verdonschot, N., Andersen,
407 M.S.J.J.o.b.e., 2015. A subject-specific musculoskeletal modeling framework to predict in vivo mechanics
408 of total knee arthroplasty. 137, 020904.

409 Martín-Hernández, C., Revenga-Giertych, C., Hernández-Vaquero, D., Albareda-Albareda, J., Queiruga-
410 Dios, J., García-Aguilera, D., Ranera-García, M., 2014. Does the medial-lateral stability of total knee
411 replacements have an effect on short-term clinical outcomes? One-year results of a multicentre study
412 with computer assisted surgery. *Revista Española de Cirugía Ortopédica y Traumatología (English Edition)*
413 58, 101-107.

414 Matsuda, S., Ito, H., 2015. Ligament balancing in total knee arthroplasty—Medial stabilizing technique.
415 *Asia-Pacific Journal of Sports Medicine, Arthroscopy, Rehabilitation and Technology* 2, 108-113.

416 Morgan, K.D., Zheng, Y., Bush, H., Noehren, B., 2016. Nyquist and Bode stability criteria to assess changes
417 in dynamic knee stability in healthy and anterior cruciate ligament reconstructed individuals during
418 walking. *Journal of biomechanics* 49, 1686-1691.

419 Nakahara, H., Okazaki, K., Hamai, S., Okamoto, S., Kuwashima, U., Higaki, H., Iwamoto, Y., 2015. Does knee
420 stability in the coronal plane in extension affect function and outcome after total knee arthroplasty? *Knee
421 Surgery, Sports Traumatology, Arthroscopy* 23, 1693-1698.

422 Ogata, K., Yang, Y., 2002. *Modern control engineering*. Prentice hall India.

423 Orozco, G.A., Tanska, P., Mononen, M.E., Halonen, K.S., Korhonen, R.K.J.S.r., 2018. The effect of
424 constitutive representations and structural constituents of ligaments on knee joint mechanics. 8, 2323.
425 Parratte, S., Pagnano, M.W., 2008. Instability after total knee arthroplasty. JBJS 90, 184-194.
426 Peng, Y., Zhang, Z., Gao, Y., Chen, Z., Xin, H., Zhang, Q., Fan, X., Jin, Z.J.M.e., physics, 2018. Concurrent
427 prediction of ground reaction forces and moments and tibiofemoral contact forces during walking using
428 musculoskeletal modelling. 52, 31-40.
429 Rasmussen, J., de Zee, M., Damsgaard, M., Christensen, S.T., Marek, C., Siebertz, K., Year A general method
430 for scaling musculo-skeletal models. In 2005 International Symposium on Computer Simulation in
431 Biomechanics, Cleveland, OH.
432 Reinders, J., Sonntag, R., Kretzer, J.P.J.B.r.i., 2014. Wear behavior of an unstable knee: stabilization via
433 implant design? 2014.
434 Rodriguez-Merchan, E.C., 2011. Instability following total knee arthroplasty. HSS journal 7, 273.
435 Sartori, M., Gizzi, L., Lloyd, D.G., Farina, D.J.F.i.c.n., 2013. A musculoskeletal model of human locomotion
436 driven by a low dimensional set of impulsive excitation primitives. 7, 79.
437 Sharifi, M., Shirazi-Adl, A., Marouane, H.J.J.o.b., 2017. Computational stability of human knee joint at early
438 stance in Gait: Effects of muscle coactivity and anterior cruciate ligament deficiency. 63, 110-116.
439 Sharifi, M., Shirazi-Adl, A., Marouane, H.J.J.o.b., 2018. Computation of the role of kinetics, kinematics,
440 posterior tibial slope and muscle cocontraction on the stability of ACL-deficient knee joint at heel strike—
441 Towards identification of copers from non-copers. 77, 171-182.
442 Sharkey, P.F., Lichstein, P.M., Shen, C., Tokarski, A.T., Parvizi, J., 2014. Why are total knee arthroplasties
443 failing today—has anything changed after 10 years? The Journal of arthroplasty 29, 1774-1778.
444 Silva, M., Shepherd, E.F., Jackson, W.O., Pratt, J.A., McClung, C.D., Schmalzried, T.P., 2003. Knee strength
445 after total knee arthroplasty¹. The Journal of Arthroplasty 18, 605-611.
446 Soeno, T., Mochizuki, T., Tanifuji, O., Koga, H., Murayama, T., Hijikata, H., Takahashi, Y., Endo, N., 2018.
447 No differences in objective dynamic instability during acceleration of the knee with or without subjective
448 instability post-total knee arthroplasty. PloS one 13, e0194221.
449 Song, S.J., Detch, R.C., Maloney, W.J., Goodman, S.B., Huddleston, J.I., 2014. Causes of instability after
450 total knee arthroplasty. The Journal of arthroplasty 29, 360-364.
451 Stoddard, J.E., Deehan, D.J., Bull, A.M., McCaskie, A.W., Amis, A.A., 2013. The kinematics and stability of
452 single - radius versus multi - radius femoral components related to Mid - range instability after TKA.
453 Journal of Orthopaedic Research 31, 53-58.
454 Thompson, J.A., Chaudhari, A.M., Schmitt, L.C., Best, T.M., Siston, R.A., 2013. Gluteus maximus and soleus
455 compensate for simulated quadriceps atrophy and activation failure during walking. Journal of
456 biomechanics 46, 2165-2172.
457 van der Krogt, M.M., Delp, S.L., Schwartz, M.H., 2012. How robust is human gait to muscle weakness? Gait
458 & posture 36, 113-119.
459 Vera-Garcia, F.J., Elvira, J.L., Brown, S.H., McGill, S.M., 2007. Effects of abdominal stabilization maneuvers
460 on the control of spine motion and stability against sudden trunk perturbations. Journal of
461 Electromyography and Kinesiology 17, 556-567.
462 Wautier, D., Thienpont, E., 2017. Changes in anteroposterior stability and proprioception after different
463 types of knee arthroplasty. Knee Surgery, Sports Traumatology, Arthroscopy 25, 1792-1800.
464 Worsley, P., Stokes, M., Taylor, M.J.G., Posture, 2011. Predicted knee kinematics and kinetics during
465 functional activities using motion capture and musculoskeletal modelling in healthy older people. 33, 268-
466 273.
467 Zaffagnini, S., Bignozzi, S., Saffarini, M., Colle, F., Sharma, B., Kinov, P.S., Marcacci, M., Dejour, D., 2014.
468 Comparison of stability and kinematics of the natural knee versus a PS TKA with a 'third condyle'. Knee
469 Surgery, Sports Traumatology, Arthroscopy 22, 1778-1785.

Table 1 Simulation parameters for BSL and WEAK models

		Baseline models	Weak models
Muscle Strength (F0) (N)	Semimembranosus	2674-2954	1800- 2530
	Semitendinosus	2674-2954	1800- 2530
	Biceps femoris	2674-2954	1800- 2530
	Rectus femoris	1260-1386	900-1188
	Vastus	6522-7200	4500-6170
	Tibialis anterior	952-1053	650-740
	Medial gastrocnemius	1568-1733	1000-1200
	Soleus	2865-3166	2000-2216
	Ligament force parameter (S0) (N)	PCL_a	8550-9450
PCL_p		8550-9450	5900-8100
MCL_a		2613-2888	1800-2475
MCL_p		2613-2888	1800-2475
MCL_i		2613-2888	1800-2475
LCL_a		1900-2100	1300-1800
LCL_p		1900-2100	1300-1800
LCL_s		1900-2100	1300-1800
MPFL		1900-2100	1300-1800
LPFL		1900-2100	1300-1800

Table 2 Anterior-posterior (A-P) displacement and internal-external(I-E) rotation for BSL and WEAK models (calculated) using FDK analysis (mean \pm std). Two different cost-functions were utilized to explore whether altered muscle recruitment strategy can mitigate the influence of defected stabilizers on knee secondary kinematics.

Variable	Baseline models		Models with weak muscles		Models with lax ligaments		Models with weak muscles and lax ligaments	
	Cost f1*	Cost f2**	Cost f1	Cost f1	Cost f1	Cost f2	Cost f1	Cost f2
A-P range(mm)	5.5 \pm 4.1	4.8 \pm 3.2	8.3 \pm 5.8	6.5 \pm 4.8	6.7 \pm 5.7	5.0 \pm 4.1	9.7 \pm 5.6	8.7 \pm 5.3
I-E range(deg)	11.6 \pm 5.7	11.2 \pm 4.5	15.7 \pm 8.4	12.9 \pm 5.5	15.3 \pm 5.4	12.5 \pm 8.2	18.4 \pm 8.5	13.8 \pm 8.4

*Costf1: Min-Max optimization

**Costf2: Synergy optimization

Appendix

Two deformable contact models were defined between the tibial insert and femoral component bearing surfaces and between the patellar button and the femoral component. The tibial insert was divided into medial and lateral compartments with separate contacts created for each. The contact force between the two objects, represented with the contacting surfaces (in STereoLithography (STL) format), was calculated using a linear force-penetration volume law.²⁹ The contact pressure module PressureModule in Newton per meter cube is the key parameter in the default FDK computational framework of AnyBody. Due to the contact model implemented in AnyBody being very close to the elastic foundation theory,²⁰ the equations derived by Fregly et al. (2003) according to the elastic foundation theory, were used for the calculation of the PressureModule :

$$\frac{p}{d} = \frac{(1 - \nu)E(p)}{(1 + \nu)(1 - 2\nu) \times h}$$

where p and d are contact pressure and surface overclosure, respectively; and $E(p)$, ν , and h are Young's modulus, Poisson's ratio, and the local thickness of the UHMWPE tibial layer, respectively; and d is the element's spring deflection, defined as the interpenetration of the undeformed surfaces in the direction of the local surface normal. For a non-linear material, the elastic modulus was set as a function of the current level of contact pressure for each element. The following equation was taken from a non-linear power law material model:

$$\varepsilon = \frac{1}{2} \varepsilon_0 \frac{p}{p_0} + \frac{1}{2} \varepsilon_0 \left(\frac{p}{p_0} \right)^n$$

where ε is the strain, p is the contact pressure, $\varepsilon_0 = 0.0597$, $p_0 = 18.4\text{MPa}$, and $n = 3$ based on the experimental stress strain data for UHMWPE (Cripton 1993). To take the derivative of p over ε , and replace with $E(p) = \frac{dp}{d\varepsilon}$, the above equation is rewritten as:

$$E(p) = \frac{1}{\left\{ \frac{1}{2} \frac{\varepsilon_0}{p_0} \left[1 + n \left(\frac{p}{p_0} \right)^{n-1} \right] \right\}}$$

Equation (3) was substituted into equation (1) to generate a single non-linear equation for p and d which was solved using a standard root-finding method. Further details for elastic foundation contact model can be found in the literature.^{3,20} In this study, the UHMWPE was considered as a non-linear material, and its elastic modulus was at least two orders of magnitude lower than that of the metallic femoral component. Therefore, the contact pressure module Pressure Module was calculated from equations (1) to (3) as a function of the contact pressure p :

$$\text{Pressure Module} = \frac{pA}{dA} = \frac{(1-\nu)}{(1+\nu)(1-2\nu)h} \times \frac{2p_0}{\varepsilon_0 \left[1 + n \left(\frac{p}{p_0} \right)^{n-1} \right]}$$

where A is the unit contact area. Due to the range of the contact pressure over the articulating surface of UHMWPE tibial inserts from 5 to 25 MPa during a gait cycle,^{31–33} the maximum, minimum, and average PressureModule values corresponding to the contact pressure values were calculated as $2.59\text{e}11 \text{ N/m}^3$, $0.48\text{e}11 \text{ N/m}^3$, and $1.24\text{e}11 \text{ N/m}^3$ respectively. Similar values for the PF joint were also adopted. The effect of using different PressureModule values on the model prediction was investigated in our previous publication (Chen et al, 2014).

References

- Chen, Zhenxian, et al. "Prediction of in vivo joint mechanics of an artificial knee implant using rigid multi-body dynamics with elastic contacts." *Proceedings of the Institution of Mechanical Engineers, Part H: Journal of Engineering in Medicine* 228.6 (2014): 564-575.
- Fregly BJ, Bei YH and Sylvester ME. Experimental evaluation of an elastic foundation model to predict contact pressures in knee replacements. *J Biomech* 2003; 36: 1659–1668
- Cripton PA. Compressive characterization of ultra high molecular weight polyethylene with applications to contact stress analysis of total knee replacements. MSc Thesis, Queen's University, Kingston, ON, Canada, 1993

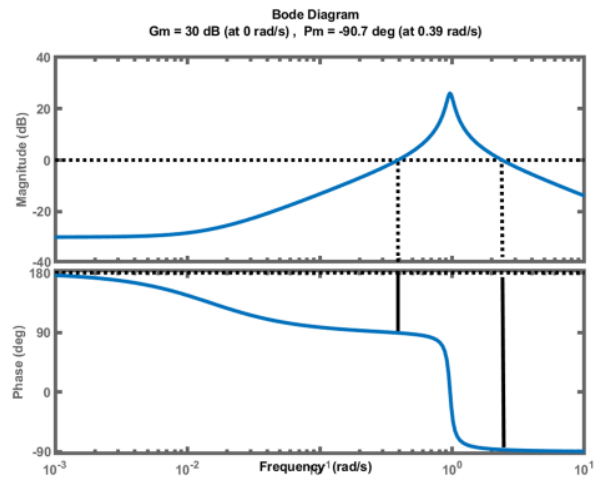
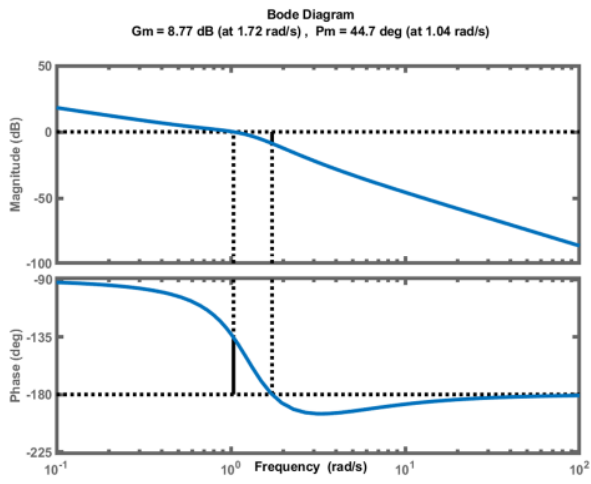


Figure A.1. Typical examples of Bode plots with positive (a) and negative (b) phase margins

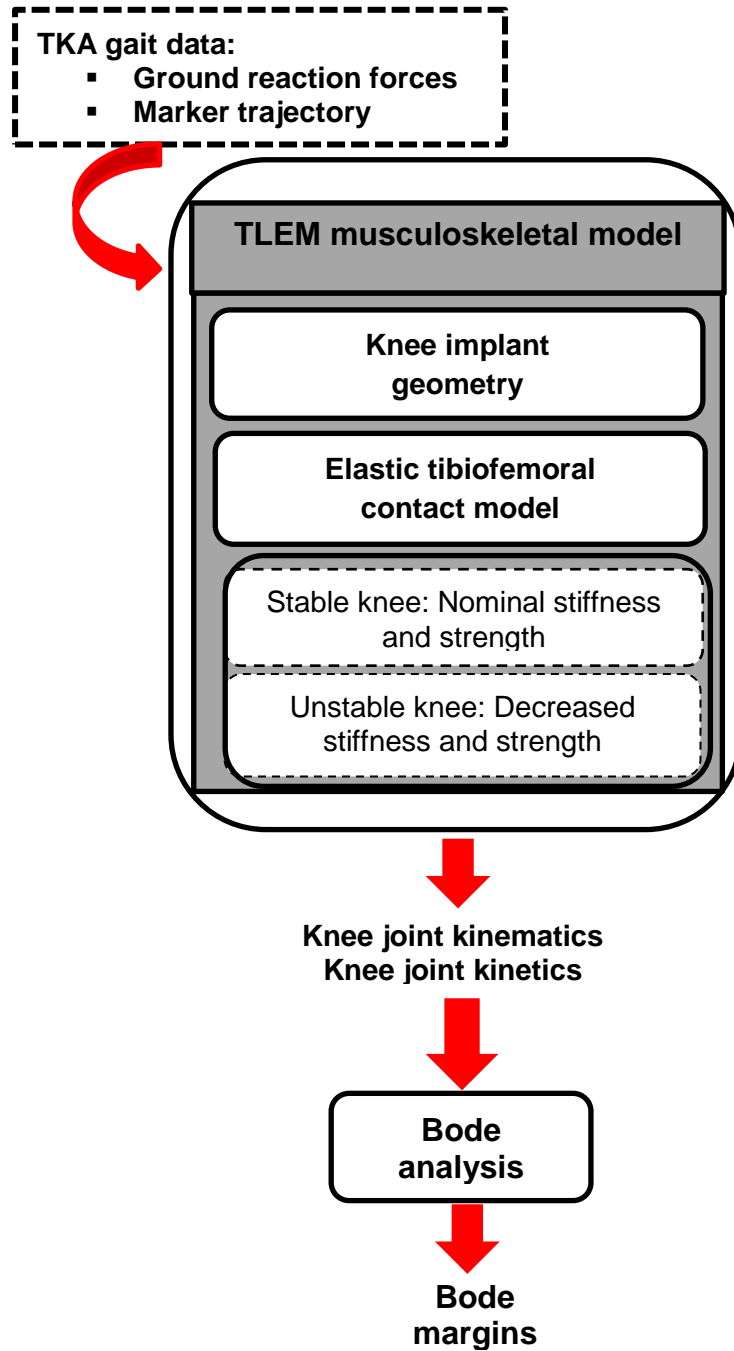


Figure 1. A schematic diagram of the modeling process used in the present study

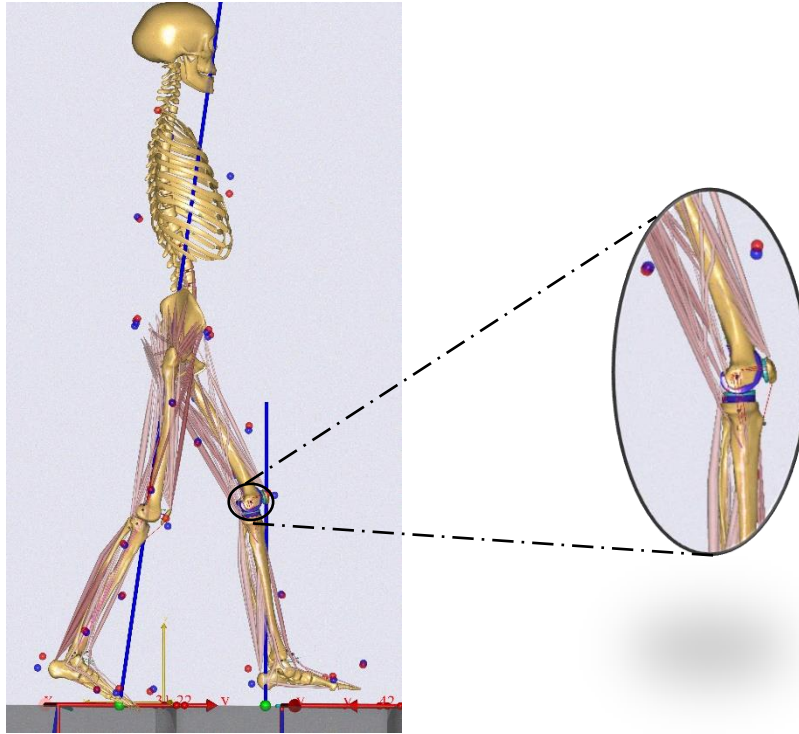


Figure 2. The TLEM MSK model was modified in AnyBody software. The geometry of knee joint was replaced with patient's implant (cruciate retaining knee implant).

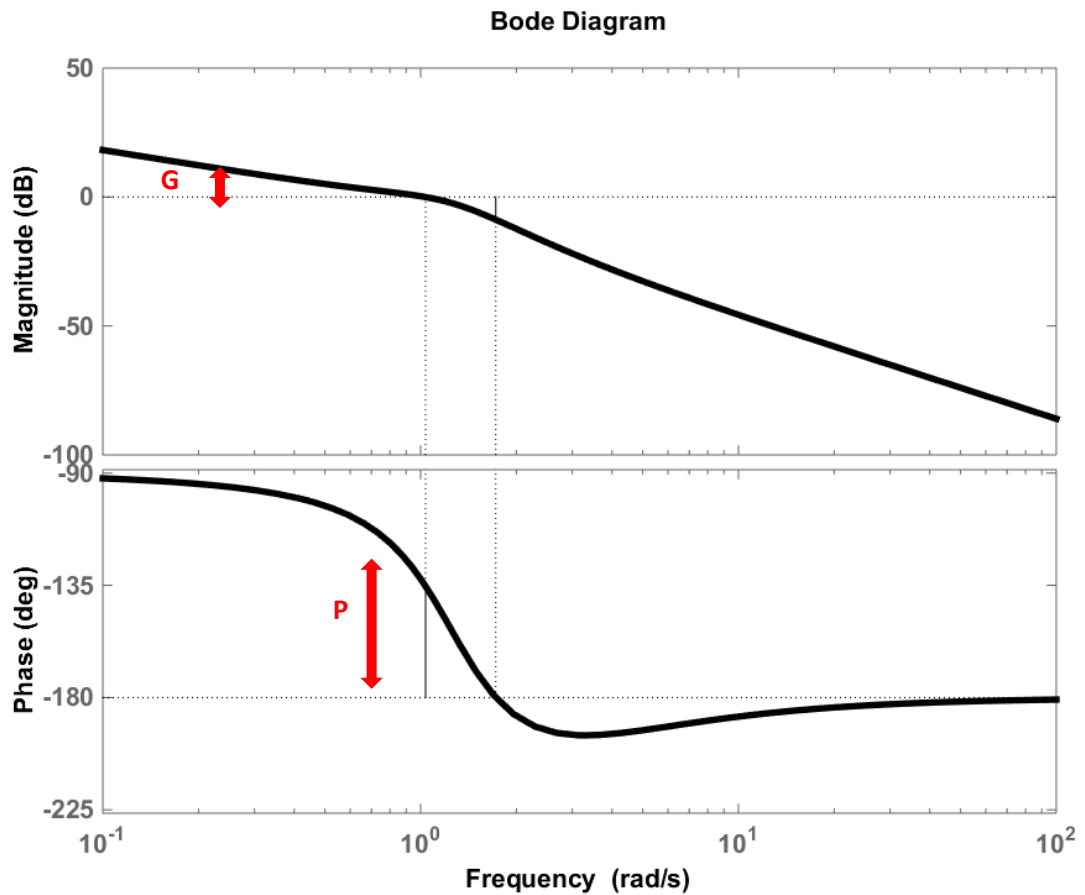


Figure 3. A typical Bode diagram to demonstrate amplitude response (G) and phase response (P) for a range of various frequencies (i.e., perturbation). The x axis demonstrates the perturbation, as the frequency of a sudden change in the inputs of knee joint model (i.e., motion and moment). The y axis in amplitude response presents the relative amplitude of knee joint power to the amplitude of perturbation. The y axis in phase response presents the time delay between when the perturbation occurs and when the peak of knee joint power is generated in response to that perturbation. Time delay is expressed in degree as gait is a periodic task and 2π radian (= 360 deg) is considered as one complete cycle delay.

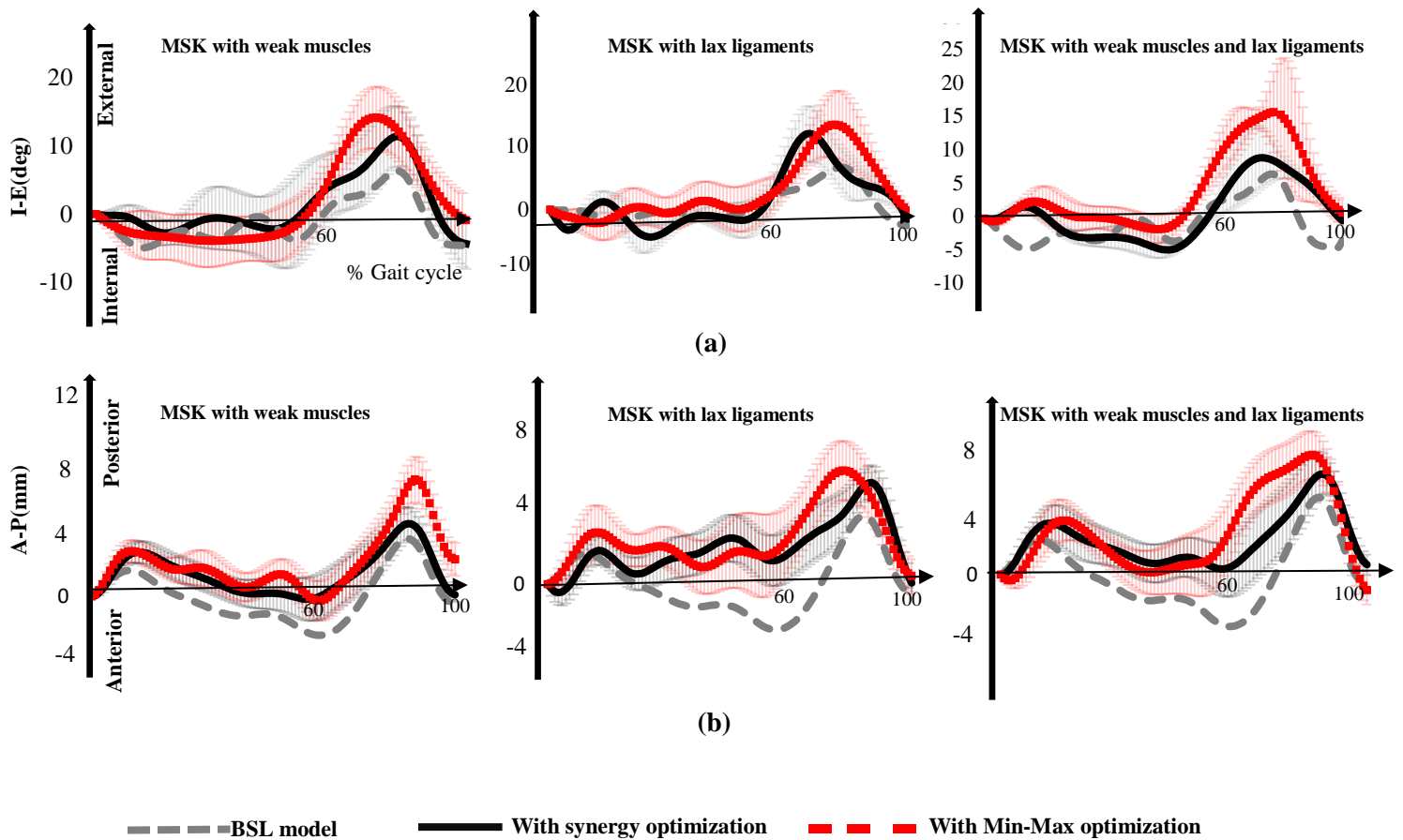


Figure 4 Internal-external (I-E) rotation (a) and anterior-posterior (A-P) displacement (b) for MSK models with weak muscles, lax ligaments and the combination of both weak muscles and lax ligaments. I-E and A-P kinematics were calculated using FDK analysis and based on two different muscle recruitment patterns: Min_Max optimization and synergy optimization. Graphs present the average and standard deviations for one representative subject.

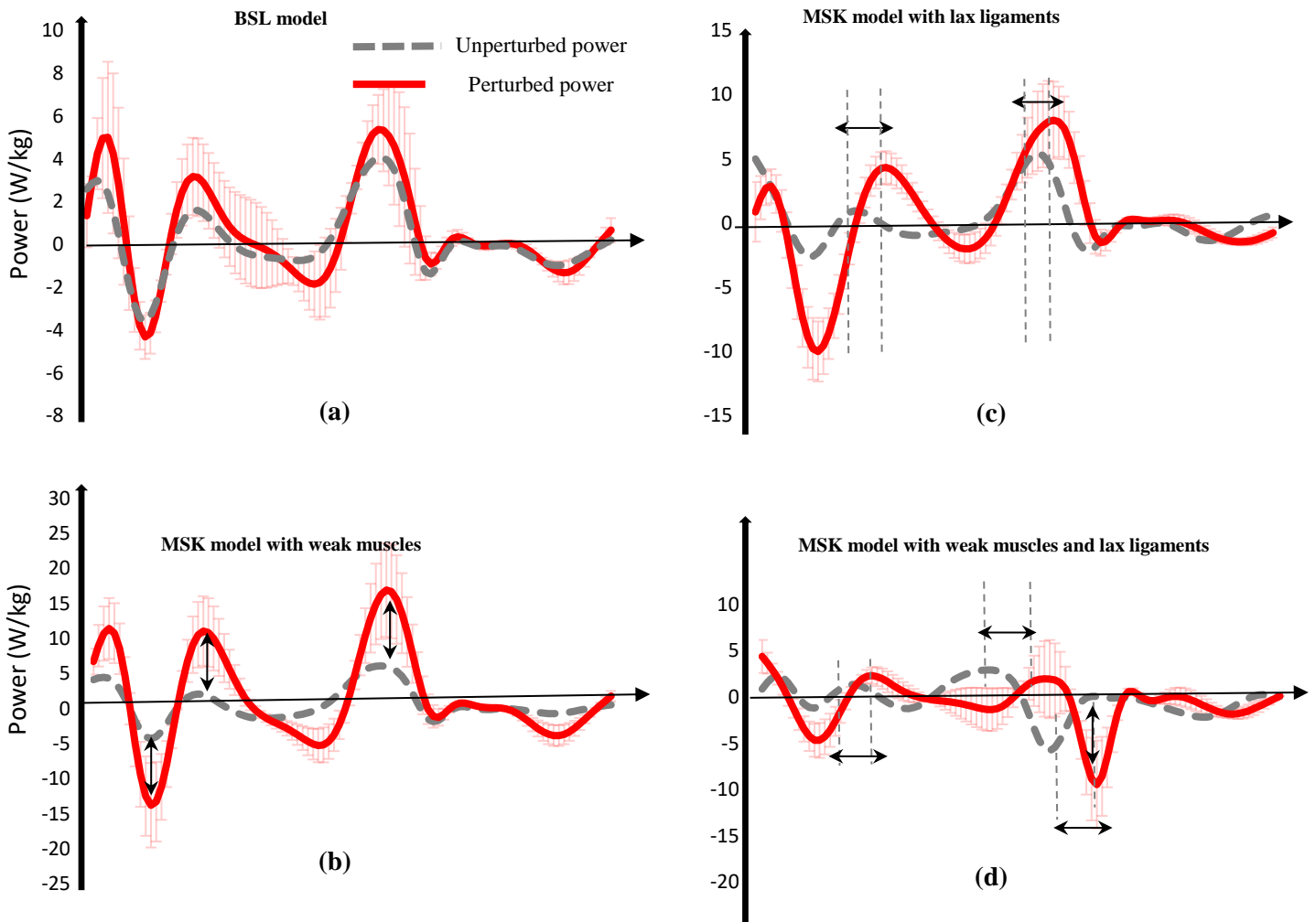


Figure 5. Comparison of perturbed knee power (calculated from Bode analysis) vs. unperturbed knee power (calculated from inverse-dynamic analysis of level-walking) for BSL models (a), models with weak muscles (b), lax ligaments (c) and models with combined deficits(d). Models with lax ligaments showed a delayed response to perturbation whilst models with weak muscles unbounded power.